



Article

# Mechanical and Microstructural Performance of Cement Mortars with Internal Carbonation and Sustainable Additives

Daria Jóźwiak-Niedźwiedzka <sup>1,\*</sup>, Paweł Lisowski <sup>1</sup>, Magdalena Osial <sup>1</sup>, Aneta Brachaczek <sup>1</sup>, Dariusz Alterman <sup>2</sup> and Alessandro P. Fantilli <sup>3,\*</sup>

- Institute of Fundamental Technological Research, Polish Academy of Sciences, Pawińskiego 5b, 02-106 Warsaw, Poland; plisowsk@ippt.pan.pl (P.L.); mosial@ippt.pan.pl (M.O.); aantolik@ippt.pan.pl (A.B.)
- School of Science, Technology & Engineering, The University of the Sunshine Coast, Sunshine Coast Mail Centre, P.O. Box 5280, Burnside, QLD 4560, Australia; dalterman@usc.edu.au
- Department of Structural, Building and Geotechnical Engineering, Politecnico di Torino, Corso Duca degli Abruzzi 24, 10129 Torino, Italy
- Correspondence: djozwiak@ippt.pan.pl (D.J.-N.); alessandro.fantilli@polito.it (A.P.F.)

#### **Abstract**

This study investigates a comprehensive study on the mechanical and microstructural behavior of cementitious mortars modified with a combination of internal carbonation (via solid CO<sub>2</sub>), calcined clay as a ceramic pozzolanic additive, and bio-based sheep wool fibers. The investigation aimed to explore sustainable routes for enhancing mortar performance while reducing the environmental impact of cement production. A series of mortars incorporating various combinations of dry ice, calcined clay, and wool fibers was prepared and tested to evaluate compressive and flexural strength, porosity, pore size distribution, phase composition, and microstructural morphology. Results demonstrated that internal carbonation significantly promoted matrix densification and compressive strength, increasing fc by approximately 8% compared to the reference. The addition of calcined clay further improved microstructural compactness, reducing total pore volume by 12%, while the incorporation of wool fibers enhanced post-cracking toughness by over 40% despite a 15-30% decrease in compressive strength. SEM and TGA confirmed the formation of calcite and reduced portlandite content, consistent with carbonation and pozzolanic reactions. The findings underscore the potential and limitations of multicomponent eco-modified cement mortars. Optimizing the balance between internal carbonation, pozzolanic reaction, and fiber stability is a key to developing next-generation low-carbon composites suitable for durable and resilient construction applications.

Keywords: internal carbonation; calcined clay; sheep wool fiber reinforcement; CO<sub>2</sub> uptake in cementitious systems; microstructural densification

# check for

Academic Editors: Gilbert Fantozzi, James G. Hemrick and Edgar Lara-Curzio

Received: 9 October 2025 Revised: 4 November 2025 Accepted: 17 November 2025 Published: 21 November 2025

Citation: Jóźwiak-Niedźwiedzka, D.: Lisowski, P.; Osial, M.; Brachaczek, A.; Alterman, D.; Fantilli, A.P. Mechanical and Microstructural Performance of Cement Mortars with Internal Carbonation and Sustainable Additives. Ceramics 2025, 8, 140. https://doi.org/10.3390/ ceramics8040140

Copyright: © 2025 by the authors. Licensee MDPI, Basel, Switzerland. This article is an open access article distributed under the terms and conditions of the Creative Commons Attribution (CC BY) license (https://creativecommons.org/ licenses/by/4.0/).

# 1. Introduction

Portland cement still remains the cornerstone of modern construction materials, even if its production accounts for approximately 7-8% of global CO<sub>2</sub> emissions [1]. In the context of increasingly stringent climate targets, research activities have been continuously proposing sustainable strategies for modifying cement-based composites in order to reduce environmental impact while maintaining, or enhancing, mechanical performance and durability. Several strategies have been developed to reduce the carbon footprint of cementitious materials, including carbon dioxide utilization through carbonation curing or internal carbonation [2,3], clinker substitution with supplementary cementitious materials

such as calcined clay or fly ash [4–7], incorporation of recycled or bio-based fibers for improved toughness [8–10], and optimization of mix design and curing conditions to reduce binder and energy demand [11–13]. Among all these approaches, internal carbonation via solid CO<sub>2</sub> (dry ice), the incorporation of supplementary cementitious materials such as calcined clays, and the use of natural fibers, such as sheep wool, as reinforcement, are the most promising. Each strategy targets a different sustainability challenge: CO<sub>2</sub> utilization through carbonation, clinker reduction via pozzolanic substitution, and circular economy implementation through biogenic fiber recycling.

Internal carbonation using dry ice has recently gained attention as an innovative in situ CO<sub>2</sub> curing method, which accelerates the formation of calcium carbonate within the cementitious matrix [3,14]. Unlike external CO<sub>2</sub> curing, which is diffusion-limited and surface-dependent, the introduction of solid CO<sub>2</sub> during mixing ensures more uniform CO<sub>2</sub> distribution and reactivity throughout the fresh mortar [2,15]. Recent studies have demonstrated that the reaction of CO<sub>2</sub> with portlandite (Ca(OH)<sub>2</sub>) leads to the precipitation of calcite, densification of the microstructure, and the increase in compressive strength at all concrete ages [16,17]. Although dry ice has a sublimation temperature of -78.5 °C, which may temporarily cool the mixture and locally freeze free water, previous studies [3,14,18] have shown that, at low dosages (≤1 wt% of binder) and short mixing times, this effect is transient and does not inhibit hydration. Internal carbonation also reduces the pH of the pore solution and promotes ettringite formation in the early hydration phase [19]. Moreover, it refines porosity by increasing the number of small, closed pores, which can enhance durability and reduce crack propagation [20]. In life-cycle terms, incorporating dry ice into fresh mortar has been reported to reduce CO<sub>2</sub> emissions per unit strength by up to 30% [21], making it a viable technique for climate-adaptive cementitious systems.

Calcined clays, especially metakaolin-rich kaolinitic clays, are increasingly being adopted as low-carbon pozzolanic additives capable of partially replacing Portland cement [4,6]. Their reactivity allows them to consume calcium hydroxide and form additional calcium silicate hydrate (C–S–H) and calcium-alumino-silicate hydrate (C–A–S–H) gels, thereby improving matrix densification and reducing permeability [5,22]. In cements, clinker replacement (up to 50%) with limestone-calcined clay (LC³) is feasible without sacrificing mechanical performance [23]. The environmental benefits are substantial, as the potential CO₂ reduction is of about 30% with respect to conventional Portland cement systems [24]. Microstructurally, calcined clays reduce total porosity and increase gel pore content, which in turn enhances resistance to chloride and sulfate ingress [25]. Furthermore, they contribute to long-term carbonation resistance by limiting CO₂ diffusion through refined pore networks, despite the initial reduction in portlandite content [26].

Natural fibers, particularly sheep wool, represent an ecological and functional alternative to synthetic or steel reinforcements [8,9,27]. These fibers are biodegradable, renewable, and often derived from waste streams of the textile and agricultural sectors. Mechanically, wool fibers improve tensile strength, post-cracking behavior, and fracture energy due to their inherent flexibility and ability to bridge microcracks [28,29]. Nonetheless, their application in cementitious environments is limited by alkaline degradation. High pH values in ordinary Portland cement matrices tend to degrade the keratin proteins in wool via disulfide bond cleavage, leading to fiber embrittlement and loss of toughness over time [30]. Strategies to improve fiber durability include surface modification (e.g., alkali treatment, plasma treatment), matrix modification via pozzolanic additives, or early carbonation to reduce alkalinity [29,31]. Pozzolanic reaction from calcined clays consumes portlandite, lowering pH and simultaneously densifying the microstructure, thus shielding fibers from aggressive pore solution exposure [4,22]. Similarly, carbonation reduces alkalinity through Ca(OH)<sub>2</sub> consumption, potentially extending fiber longevity [16,17,32].

While previous studies have independently addressed internal carbonation, calcined clay substitution, and natural fiber reinforcement in cementitious mortars [4,33–36], there remains a lack of systematic investigation into their combined interactions, particularly with respect to microstructure–chemistry compatibilities and fiber durability under altered alkalinity conditions. This study therefore hypothesizes that the synergy between internal carbonation and calcined clay will enhance densification, but that fiber reinforcement may become compromised by concurrent changes in pore solution chemistry. For example, carbonation-induced pH reduction may enhance fiber stability, but this effect could simultaneously interfere with pozzolanic reactions or lead to undesirable porosity. Similarly, fibers may disrupt CO<sub>2</sub> diffusion or alter hydration kinetics.

Accordingly, the present study aims to fill this knowledge gap by comprehensively evaluating the mechanical and microstructural performance of cement mortars when they are modified by a simultaneous presence of dry ice (as a source of internal carbonation), calcined clay (as a pozzolanic additive), and sheep wool fibers (as natural reinforcement). Through tests on mechanical performance, pore structure, phase composition, and microstructural morphology, this study investigates how all the components interact and whether their combination can deliver multifunctional, low-carbon composites for structural applications. The findings are expected to advance the development of next-generation eco-efficient mortars that align with the principles of durability, performance, and environmental responsibility in modern constructions.

# 2. Materials and Methods

#### 2.1. Materials

The mortar components were selected to balance sustainability, reactivity, and structural performance. The reference binder was Ordinary Portland Cement CEM I 42.5R, which exhibited a specific surface area of  $4.10~\rm m^2/g$  and a typical chemical composition, including 63.1% CaO, 19.5% SiO<sub>2</sub>, and 4.8% Al<sub>2</sub>O<sub>3</sub> (see Figure 1).

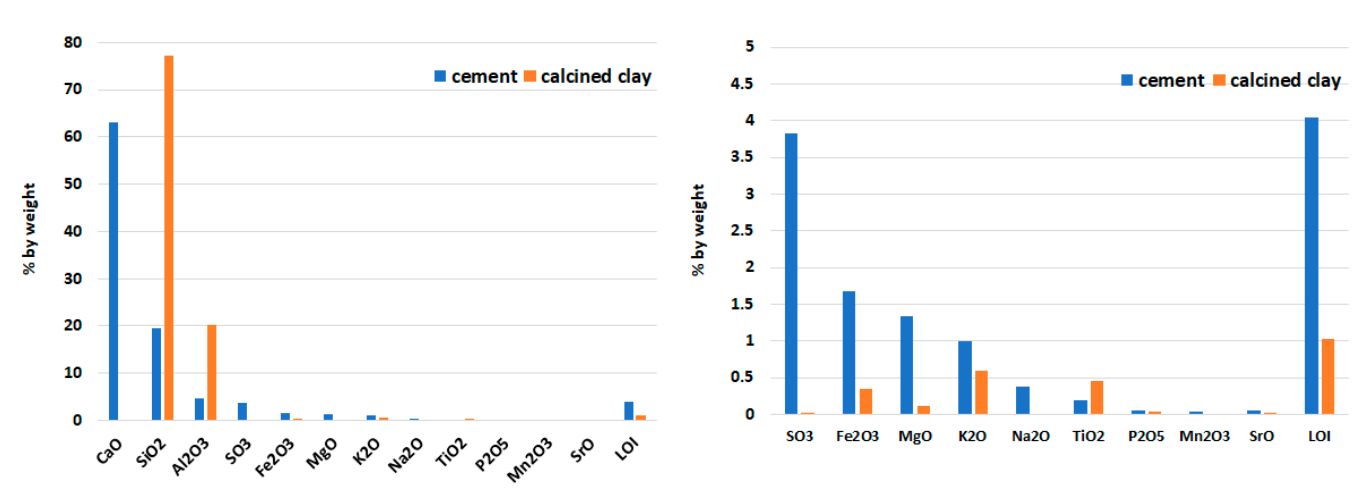


**Figure 1.** Chemical composition of cement and calcined clay determined by XRF analysis; major components and trace components expressed as wt%, including loss on ignition (LOI).

Calcined clay was employed as a supplementary cementitious material and constituted 15% or 30% of the total binder in selected mixtures. It was produced by thermal activation of kaolinitic clay, yielding a highly reactive material with a BET surface area of  $17.48 \text{ m}^2/\text{g}$ .

Natural sheep wool fibers, collected and cleaned to remove surface oils, were cut into 16 mm lengths with an average diameter of 20  $\mu$ m. These biodegradable fibers are known for their ability to bridge cracks and delay crack propagation. However, they are also susceptible to alkaline degradation, which was a focus of this investigation [9,28].

Ceramics **2025**, 8, 140 4 of 19

Solid carbon dioxide (dry ice) was used in pellet form (Ø 3 mm, length  $\sim$ 16 mm) to induce internal carbonation during mixing. The pellets sublimated rapidly, releasing CO<sub>2</sub> uniformly within the matrix and reacting with portlandite to form calcite.

Fine standard siliceous sand (0–2 mm) and tap water were used as aggregate and mixing fluid, respectively. All materials were used in accordance with EN 196-1 [37] specifications.

# 2.2. Mix Design

To comprehensively assess the effects of combining calcined clay, internal carbonation, and natural fiber reinforcement, eight distinct mortar formulations were systematically developed, as outlined in Table 1. The design strategy was based on an approach to isolate the contribution of each component to understand how their coexistence influences both mechanical and microstructural outcomes.

Mortar	CEM I	Calcined Clay	Sand Water		Dry Ice	Wool Fibers
M1	450	_	1350	225	-	_
M2	450	_	1350	225	6.75	_
M3	450	_	1350	225	-	10
M4	450	_	1350	225	6.75	10
M5	315	135	1350	225	_	_
M6	315	135	1350	225	6.75	_
M7	315	135	1350	225	_	10
M8	315	135	1350	225	6.75	10

**Table 1.** Composition of the mortars (g/L).

To ensure consistency across the mixture, all the mortars were prepared with a constant sand-to-binder ratio of 3:1 and a fixed water-to-binder ratio of 0.5. Components were mixed in a high-shear laboratory mixer, in which dry ice, dosed at 1.5% of the total binder mass, was introduced in the final step and mixed for an additional 60 s to prevent premature sublimation. This approach is consistent with the procedures reported by Xuan et al. [3], who also emphasized short mixing times and immediate casting to minimize  $CO_2$  loss and thermal effects.

Fresh mortar was poured into standardized prismatic molds ( $40 \times 40 \times 160 \text{ mm}^3$ ) in two layers. A mechanical compaction was applied to minimize entrapped air. The molds were finally covered with plastic sheets to prevent early moisture loss. After 24 h of curing at ambient temperature, the specimens were demolded and immersed in a pool with water at  $20 \pm 1$  °C, where they remained for 28 days to ensure complete hydration and phase development prior to testing.

#### 3. Methods

Mechanical performances were evaluated through flexural and compressive tests, performed in accordance with EN 196-1 [37]. More precisely, flexural strength was measured in prismatic mortar specimens ( $40 \times 40 \times 160 \text{ mm}^3$ ) tested in three-point bending by using a displacement-controlled universal testing machine (maximum load capacity of 500 kN). A constant crosshead displacement rate of 0.06 mm/min was applied until the failure. The test setup allowed real-time recording of both load and mid-span deflection to determine flexural strength ( $f_t$ ) and post-cracking flexural toughness. Toughness was quantified by integrating the area under the load–deflection curve up to a relative displacement (the net displacement after the peak) of 0.03 mm.

Ceramics **2025**, 8, 140 5 of 19

After the flexural strength test, the two halves of each prism were used for compressive strength determination in accordance with EN 196-1 [37]. The compressive load was applied to the intact surfaces, away from the flexural crack, ensuring that the prior fracture did not affect the measured strength values. Each half was subjected to a uniaxial compression test by means of a 500 kN capacity hydraulic press. Load was applied at a rate of  $2.4 \, \text{kN/s}$  until failure, at which compressive strength ( $f_c$ ) is measured. Five specimens per mix were tested in compression and three in flexure, to ensure statistical validity, following standard recommendations.

The remaining halves of the prisms were used to perform other tests, such as the thermogravimetric analysis (TGA) using a PerkinElmer TGA 8000 instrument (PerkinElmer Inc., Waltham, MA, USA). Approximately 40 mg of powdered mortar (sieved < 45  $\mu m$ ) was heated from room temperature to 1000 °C, at a rate of 10 °C/min, under a nitrogen atmosphere to prevent external carbonation. The measurements were performed using ceramic crucible under the  $N_2$  atmosphere at a gas flow rate of 40 mL/min. Key mass loss intervals were used to determine quantities of ettringite (50–120 °C), monosulfate (120–200 °C), portlandite (400–550 °C), and calcium carbonate (550–750 °C).

Specific surface area and pore structure were analyzed using the Brunauer–Emmett–Teller (BET) method. A Quantachrome Autosorb IQ analyzer (Quantachrome Instruments, Boynton Beach, FL, USA) was used, with  $N_2$  as adsorber. Powdered specimens were degassed at 105 °C for 16 h under vacuum. The analysis consisted of 25 adsorption and 20 desorption points over a relative pressure range from 0.05 to 1.0 (p/p<sub>0</sub>). The BET surface area and BJH pore distribution were derived using multipoint analysis.

Alkalinity of the pore solution was evaluated by suspending 20 g of finely ground mortar (sieved < 45  $\mu$ m) in 20 mL of deionized water. The slurry was magnetically stirred for 5 min and then allowed to settle. Measurements were taken using a calibrated digital pH meter equipped with a microelectrode. Calibration was performed with pH buffers at 7.00, 9.21, and 11.00, and three measurements per each specimen were taken.

The microstructure of fractured mortar specimens was examined using a scanning electron microscopy (SEM) in secondary electron mode, coupled with energy-dispersive X-ray spectroscopy (EDS) for elemental mapping. A JEOL JSM-6380 microscope (JEOL Ltd., Akishima, Tokyo, Japan) operated at 15 kV with an 8 mm working distance. Specimens were mounted on carbon tape and carbon-coated to improve surface conductivity. Particular attention was given to the morphology of hydration products, carbonation by-products, and fiber integrity within the matrix.

#### 4. Results

#### 4.1. Characterization of Raw Materials

The chemical and microstructural characteristics of the raw materials are presented in Figures 1–3. According to the XRF analysis (Figure 1), the calcined clay consisted predominantly of silica ( $SiO_2 = 77.1$  wt%) and alumina ( $Al_2O_3 = 20.2$  wt%), confirming its pozzolanic nature and potential reactivity with portlandite during hydration and carbonation processes.

The SEM observations (Figure 2) revealed that the calcined clay particles exhibited a porous and lamellar morphology, which favors mechanical interlocking and enhances the surface area available for chemical reactions. The wool fibers displayed a scaly surface texture typical of keratin-based materials, promoting good adhesion to the cementitious matrix. For reference, the morphology of the dry ice pellets used for internal carbonation is also shown, highlighting their compact granular structure that facilitates uniform CO<sub>2</sub> release within the mix.

Ceramics **2025**, 8, 140 6 of 19

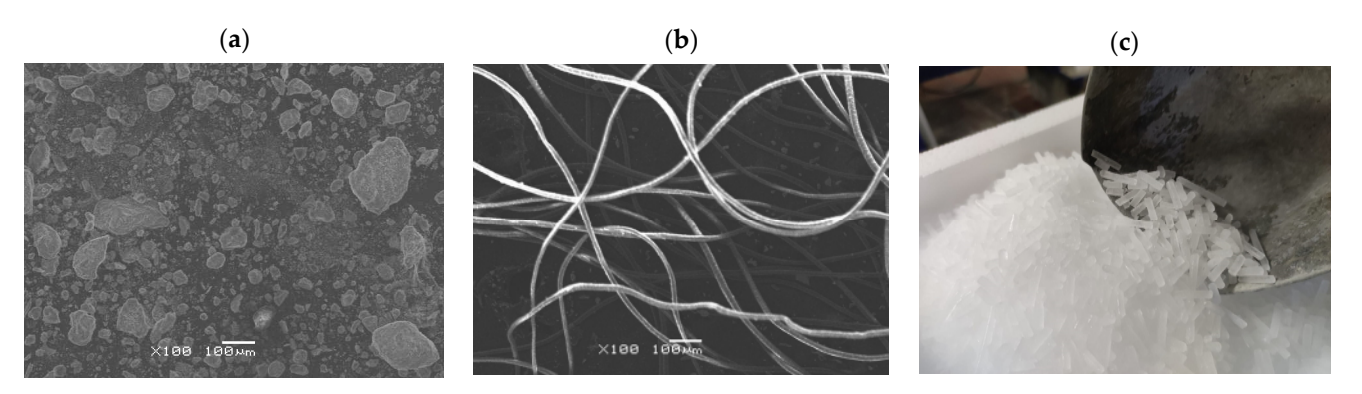


Figure 2. Microphotographs of the: (a) calcined clay, (b) sheep wool fiber, (c) dry ice pellets.

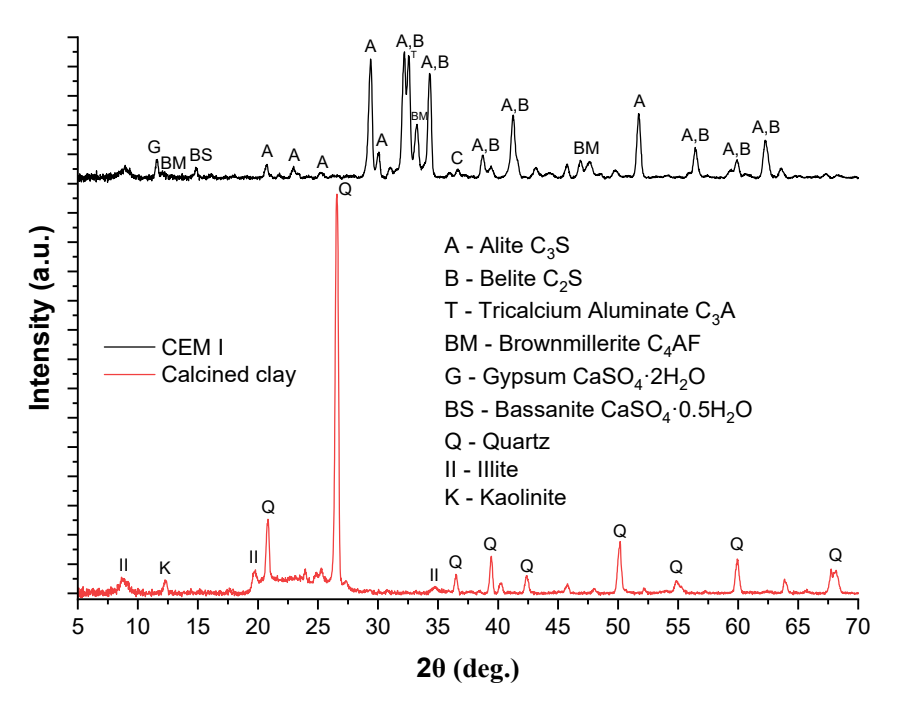


Figure 3. XRD patterns of CEM I and calcined clay.

The mineralogical composition of the cement and calcined clay was analyzed using XRD (Figure 3). The diffraction pattern of the Portland cement CEM I 42.5R displayed sharp reflections corresponding to alite ( $C_3S$ ), belite ( $C_2S$ ), tricalcium aluminate ( $C_3A$ ), and tetracalcium aluminoferrite ( $C_4AF$ ), confirming a high degree of crystallinity typical of hydraulic clinker phases responsible for early strength development. In contrast, the XRD profile of the calcined clay was characterized by a broad diffuse hump between  $20^\circ$  and  $30^\circ$   $2\theta$ , indicative of an amorphous aluminosilicate structure formed during dehydroxylation of kaolinite. Residual crystalline peaks of quartz and mullite were also identified, suggesting that the thermal activation led to partial, rather than complete, transformation of the kaolinitic precursors.

#### 4.2. Mechanical Properties

The average values of the compressive and flexural strength of cement mortars are presented in Figure 4, whereas those of the flexural toughness  $A_F$  are shown in Figure 5. The mechanical performance varied significantly across the different mortar formulations (Table 1, Figure 4). The reference mix (M1) reached a compressive strength of 44 MPa and a flexural strength of 4.05 MPa. Internal carbonation produced by the addition of dry ice (M2) increased the compressive strength up to 47.5 MPa. Flexural strength in M2 (4.15 MPa) also improved slightly with respect to M1. The inclusion of only wool fibers (M3) further

Ceramics **2025**, 8, 140 7 of 19

enhanced flexural strength to 4.9 MPa, though compressive strength dropped to 38 MPa. When both dry ice and fibers were added (M4), the performance in bending remained high (flexural strength equal to 4.75 MPa), while compressive strength remained almost the same (39 MPa). In the mixtures incorporating calcined clay, compressive strength ranged from 43 MPa to 47 MPa. However, the addition of wool fibers to these mortar systems (M7) led to low compressive strength (37 MPa) but sustained high flexural strength (4.80 MPa). The full combination (M8) showed the poorest mechanical results, with both compressive and flexural strength decreasing to 30 MPa and 4.0 MPa, respectively.

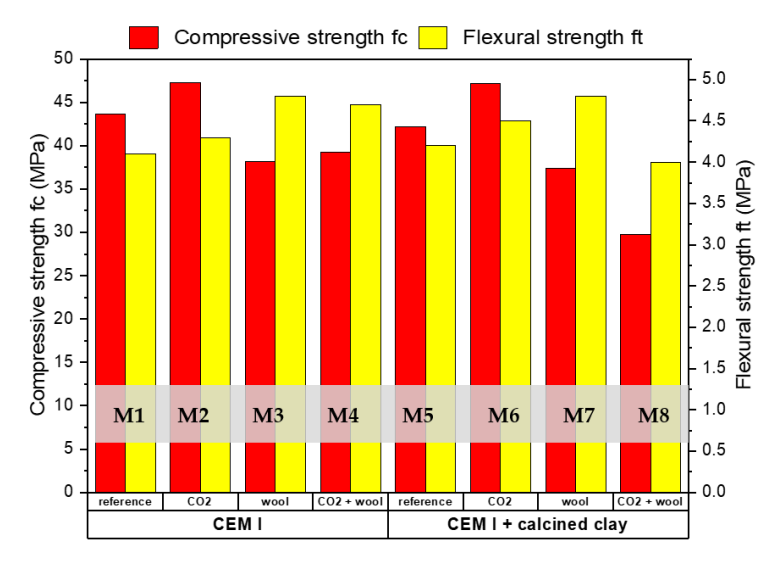


Figure 4. Average values of compressive and flexural strength.

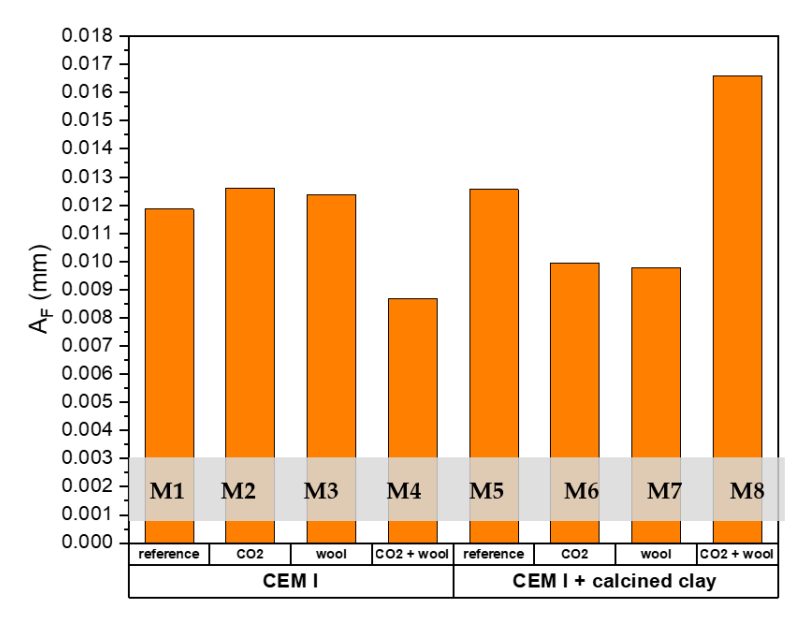


Figure 5. Average values of flexural toughness.

Flexural toughness, assessed via average deflection after cracking, was significantly influenced by fiber content (Figure 5). The highest toughness was observed in M3 ( $A_F = 0.023 \text{ mm}$ ), validating the role of wool fibers in enhancing post-crack energy absorption., Despite the low strength, M8 demonstrated the highest  $A_F$  (0.030 mm), likely due to matrix degradation and high porosity. Mortars without fibers exhibited the lowest  $A_F$  values, in particular M5, in which  $A_F = 0.0087 \text{ mm}$ .

Ceramics **2025**, 8, 140 8 of 19

## 4.3. Thermogravimetric Analysis

Thermogravimetric analysis (TGA) was conducted to quantify the relative amounts of some hydration and carbonation products within the hardened mortar specimens. Figure 6 illustrates the calculated weight-based contents of portlandite, calcite, ettringite, and monosulphate across all the mortar variants.

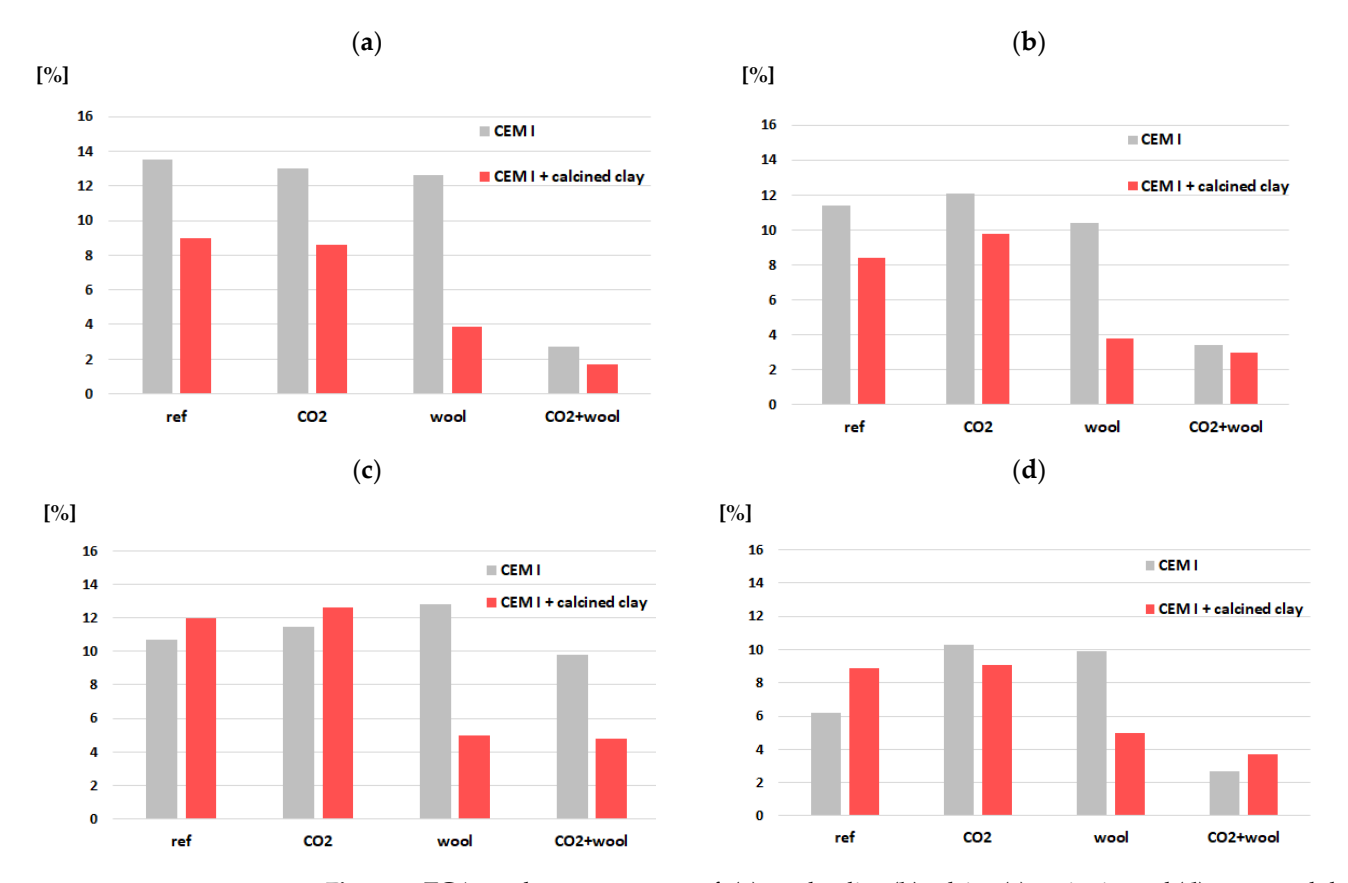


**Figure 6.** TGA results—percentages of: (a) portlandite, (b) calcite, (c) ettringite and (d) monousulphate in the mortars investigated herein.

The highest portlandite content (13.5%) was recorded in the reference mortar (M1), indicating a typical degree of hydration of plain Portland cement paste. In contrast, a low content of portlandite was observed in the mixtures modified with dry ice and/or calcined clay. Notably, mix M8, incorporating dry ice, calcined clay, and wool fibers, exhibited the lowest  $Ca(OH)_2$  content (1.7%), suggesting an extensive consumption via both carbonation and pozzolanic reaction mechanisms. These results are consistent with the combined effect of  $CO_2$ , reacting with portlandite to form calcite, and the pozzolanic activity of calcined clay, consuming available calcium hydroxide during secondary gel formation.

Calcite formation followed an inverse trend. The highest calcite content (12.1%) was observed in mix M2 (dry ice only), confirming the effectiveness of internal carbonation in situ. Moderate calcite levels were noted in partially modified systems, while mix M8 demonstrated a reduced calcite content (3.0%) despite the presence of  $CO_2$ . This reduction may be attributed to competitive reactions, limited  $CO_2$  availability due to pore refinement, or fiber-induced diffusion barriers, and an overlapping pozzolanic consumption of calcium hydroxide.

Ettringite formation varied considerably among the compositions. Mix M3 (wool fibers only) showed the highest ettringite content (12.8%), likely due to unaltered early-age sulfate reaction pathways. In contrast, mortar mixtures subjected to internal carbonation (e.g., M2, M4, M8) displayed significantly lower ettringite contents, ranging from 4.8%

Ceramics **2025**, 8, 140 9 of 19

to 7.6%. This is due to the fact that carbonation-induced pH reduction and portlandite depletion limit the stability of AFt phases. Pozzolanic substitution also influenced ettringite availability, likely due to alumina incorporation into other hydration products.

Monosulphate content exhibited a generally decreasing trend in the modified mortars, with the lowest value again observed in mortar M8. These data imply that carbonation and pozzolanic reaction not only reduce portlandite but also influence the equilibrium among sulfate-bearing phases. The transformation of monosulphate into other products under modified pH and Ca availability conditions may contribute to the overall reduction in AFm phases.

#### 4.4. Pore Structure and BET Surface Area Analysis

Figures 7–9 present the BET surface area, total pore volume, and gel pore distribution for all the mortars. The highest surface area  $(13.0 \text{ m}^2/\text{g})$  and total pore volume  $(0.114 \text{ cm}^3/\text{g})$  were observed in mix M7 (calcined clay + wool), reflecting increased porosity due to the presence of fibers. In contrast, mortars containing dry ice (M2, M4, M6) and/or calcined clay without fibers (M5, M6) exhibited lower surface areas and pore volumes, indicating effective matrix densification via carbonation and pozzolanic reactions. Gel pore content (<10 nm) was highest in M5 (54%), confirming the pore-refining effect of calcined clay. The lowest gel pore content (38.96%) was observed in M8, consistent with chemical incompatibilities and structural disruption caused by the combined presence of carbonation, pozzolanic additives, and fibers.

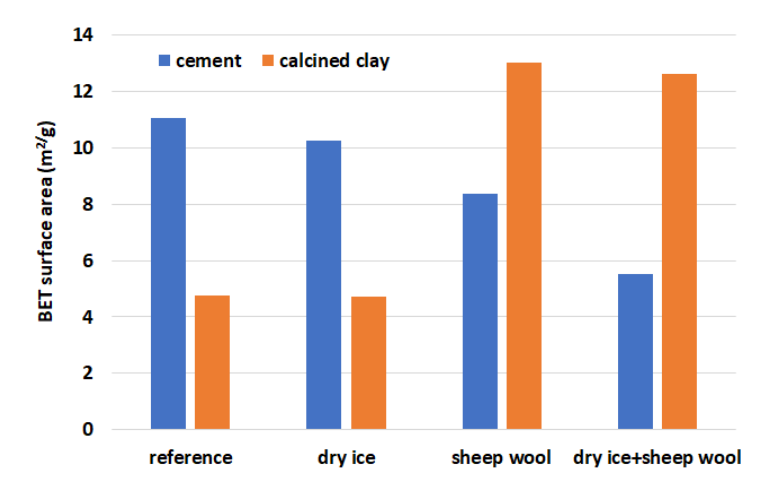


Figure 7. BET surface area.

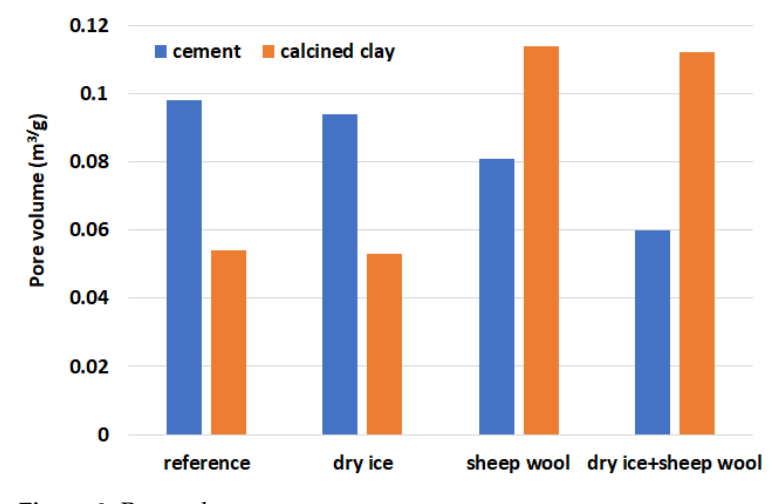


Figure 8. Pore volume per mortar.

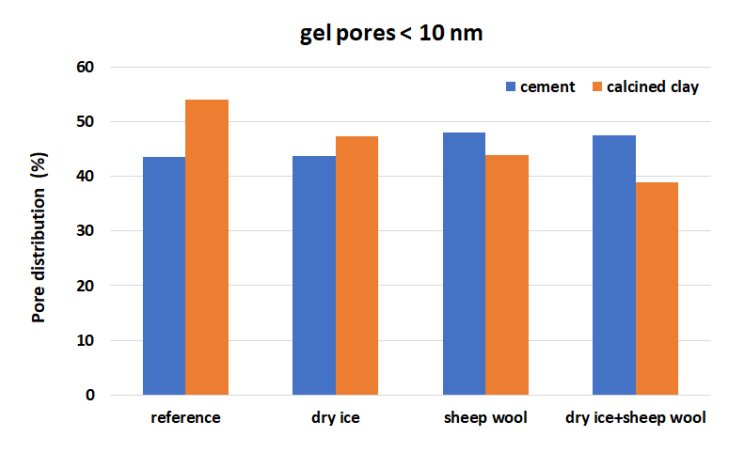
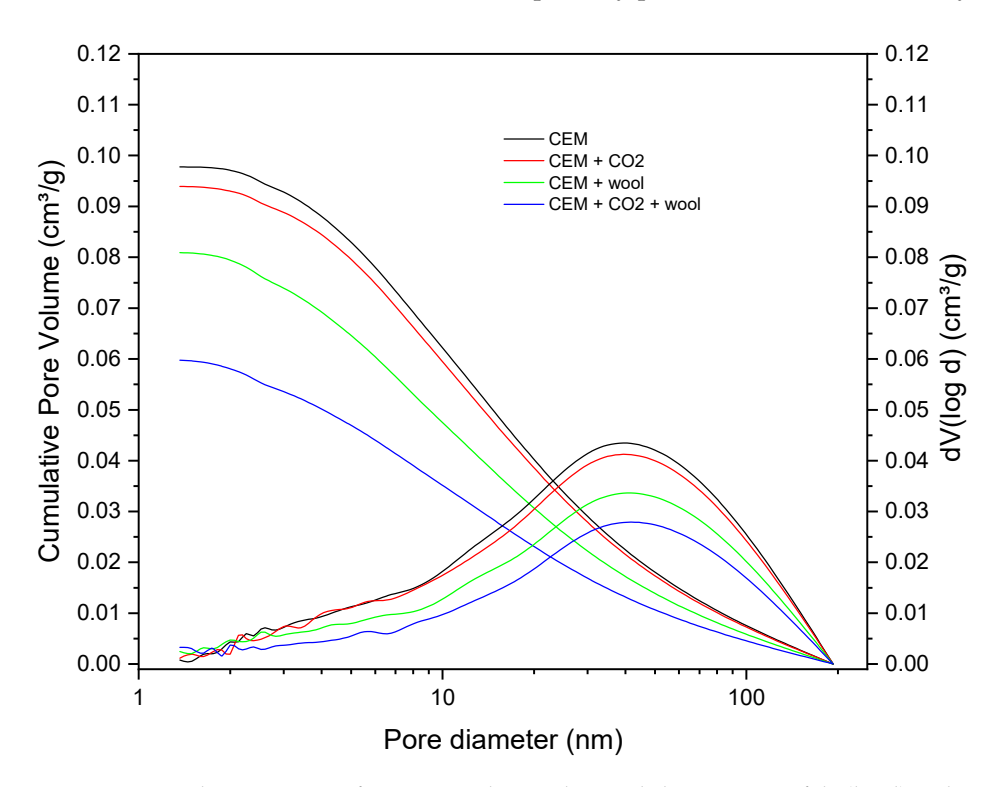
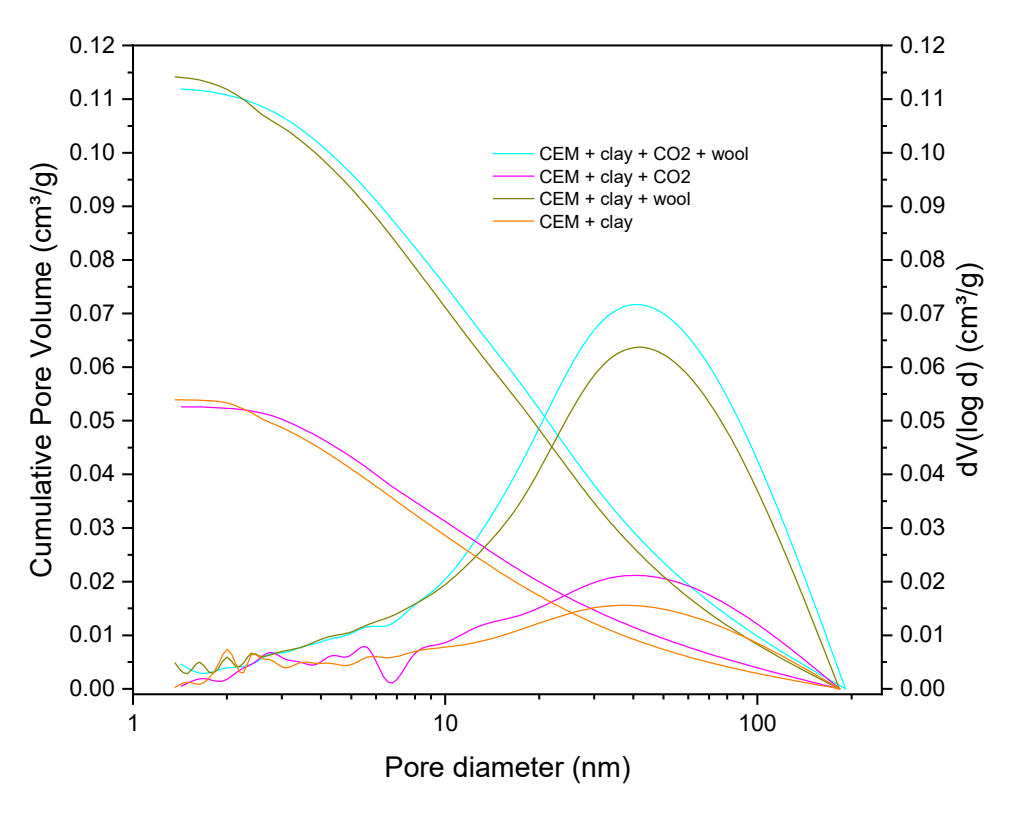


Figure 9. Gel pores characteristics.

Figures 10 and 11 present pore volume distributions for all mortar compositions and the cumulative values. The results confirm that internal carbonation (dry ice) and pozzolanic substitution (calcined clay) significantly refine the pore structure. In mortars with calcined clay (Figure 11), a shift toward smaller pore diameters was evident, particularly in mortar M5, where the cumulative pore volume increased more gradually with pore size—indicating higher gel pore content. Conversely, mortars containing wool fibers, especially M7 and M8, displayed broader pore distributions, because meso- and macroporosity increased due to fiber-induced voids. The combined presence of carbonation and clay (M6 and M8) resulted in bimodal distributions, probably produced by an interaction between densification and structural disruption. Overall, M5 had the most refined pore network, while M8 demonstrated the least favorable porosity profile in terms of durability.



**Figure 10.** Pore characteristics of mortars without calcinated clay in terms of dV(logd) and cumulative pore volume.



**Figure 11.** Pore characteristics of cement mortars with calcined clay in terms of dV(logd) and cumulative pore volume.

# 4.5. Alkalinity of Mortars

As shown in Table 2, in all the mortars, pH varied within the range 12.0–12.5, revealing the typical high alkalinity of cementitious materials. The reference mixture (M1) and those containing only wool reinforcement (M3) recorded the highest pH values (12.5), reflecting the presence of free portlandite and unaltered hydration products. In contrast, mortars with dry ice (i.e., M2, M4, M6, and M8) showed slightly reduced pH (12.4–12.0) due to the consumption of Ca(OH)<sub>2</sub> during carbonation. Similarly, in the presence of calcined clay (i.e., M5, M6, M7, and M8), pH is lower (12.3–12.0), which can be attributed to pozzolanic reaction and the reduction in free hydroxides. The lowest pH (12.0) was measured in M8, where carbonation and pozzolanic activity acted synergistically, resulting in a more neutral environment compared to the reference mortar.

Table 2. The pH values measured in all the mortars.

M1	M2	М3	M4	M5	M6	M7	M8
12.5	12.4	12.5	12.1	12.3	12.2	12.1	12.0

#### 4.6. Microstructure

SEM analysis (shown in Figures 12 and 13) revealed significant differences in the microstructural morphology and fiber integrity among the mortars containing sheep wool fibers. In the reference fiber-reinforced mortar (M3), composed of CEM I and wool fibers, intact portlandite crystals were observed alongside partially degraded fibers. Such a situation is due to the typical alkaline-induced deterioration of wool in a high-pH environment. The addition of dry ice (M4) resulted in a distinct microstructure characterized by dispersed calcite crystals and the absence of portlandite, confirming the occurrence of internal carbonation. In this matrix, wool fibers showed high degradation, suggesting that carbonation further compromised fiber stability. Mortars incorporating calcined clay (M7) displayed

denser microstructures with visible fiber morphology largely preserved. It can be attributed to the pozzolanic reaction, which lowers the pH and moderates the chemical aggressiveness of the environment. However, in the most complex system (M8), where dry ice, calcined clay, and wool fibers were combined, SEM images revealed severe fiber degradation, with only residual outlines remaining.

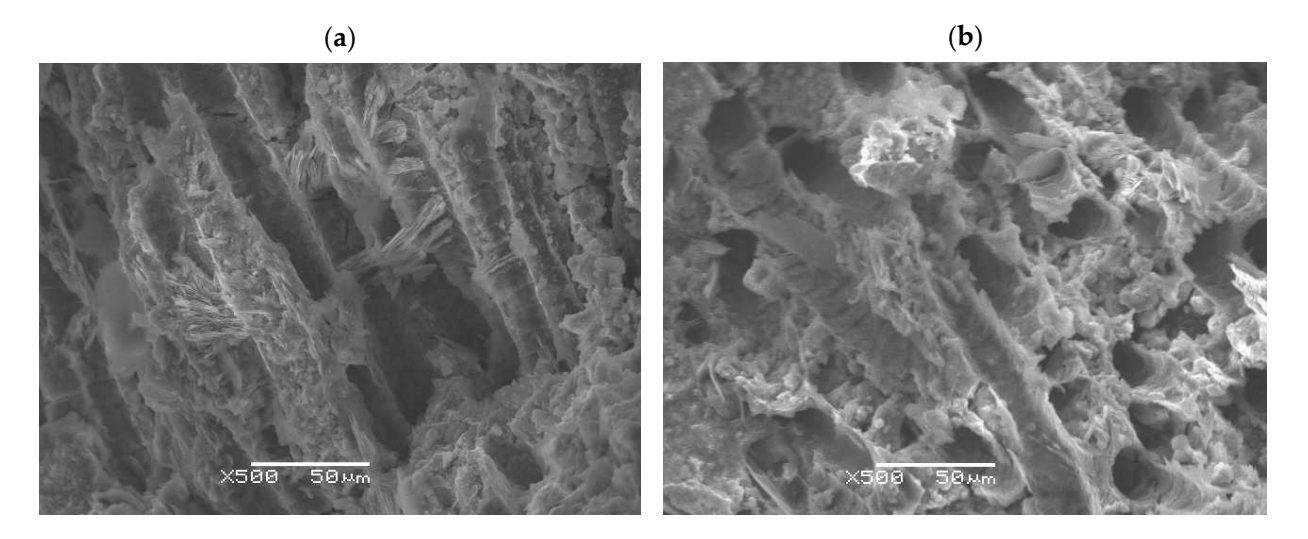


**Figure 12.** The SEM microstructure of mortars with sheep wool fibers observed on split surfaces: (a) M3—CEM I + wool and (b) M4—CEM I + wool + CO<sub>2</sub>.

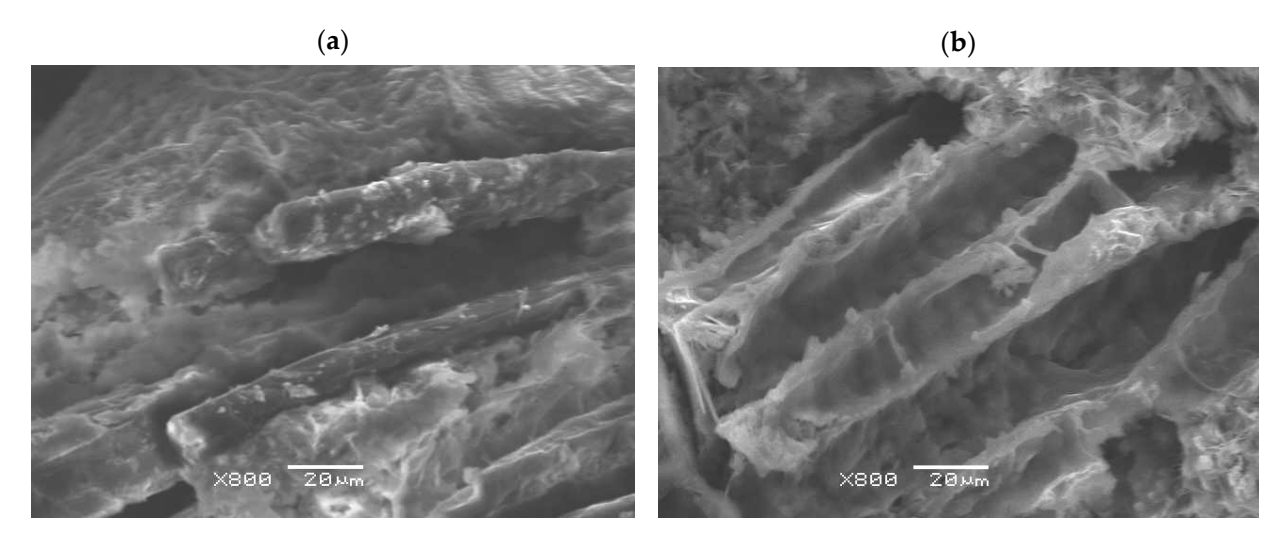


**Figure 13.** The SEM microstructure of mortar with sheep wool fibers observed on split surfaces: (a) M7—CEM I + calcined clay + wool and (b) M8—CEM I + calcined clay + wool + CO<sub>2</sub>.

Figure 14 shows the SEM microstructure of mortar M8 (CEM I + calcined clay + wool +  $CO_2$ ) with EDS analysis, which confirms the presence of calcite crystals. The observed crystalline phase is characterized by high calcium content, consistent with carbonation products formed through the reaction of  $CO_2$  with portlandite. Moreover, this confirms the internal carbonation in the modified matrix.

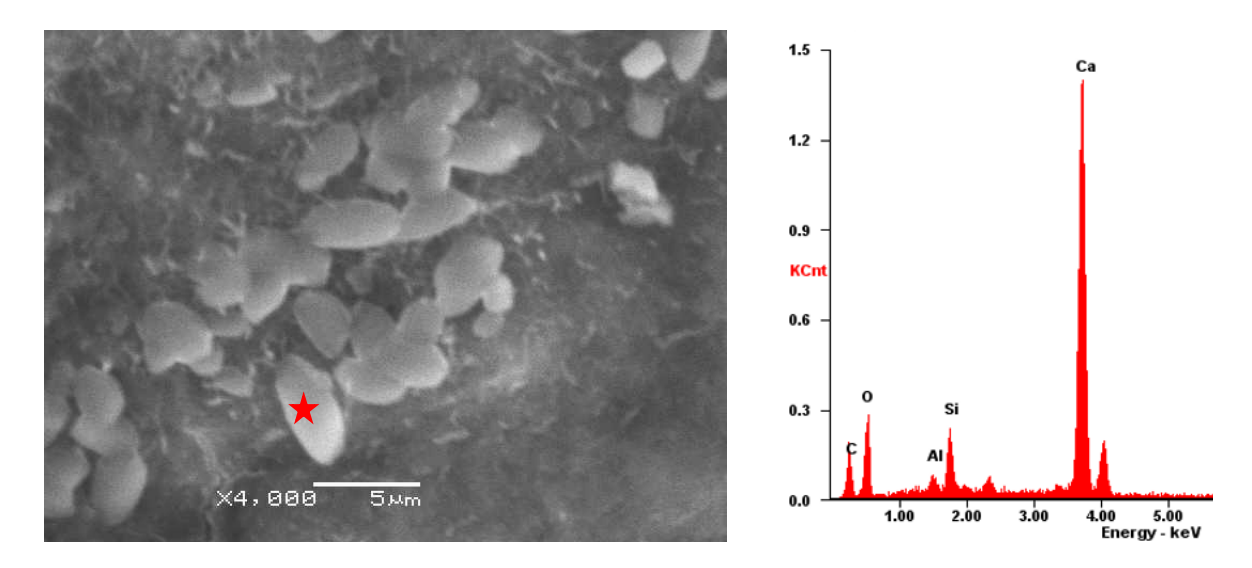


Figure 14. The SEM microstructure of mortar M8 (CEM I + calcined clay + wool +  $CO_2$ ) with EDS analysis confirming the presence calcite crystals.

# 5. Discussion

The results shown in the previous sections demonstrated the complex interplay between internal carbonation via dry ice, pozzolanic activity from calcined clay, and fiber reinforcement with sheep wool fiber, when Fiber-induced diffusion barriers and competing pozzolanic reactions in multicomponent blends used in cementitious mortars. It is possible to observe that while each modification individually improves specific aspects of performance, their combination requires careful balance to avoid conflicting effects. This highlights the importance of understanding the coupled chemical–microstructural processes that govern mechanical performance and durability in multi-component sustainable mortars.

The incorporation of dry ice as a means of internal carbonation significantly increased early-age compressive strength, according to previous findings that carbonation promotes matrix densification through calcite precipitation [2,38,39]. TGA results and SEM-EDS analysis (Figure 14) revealed the formation of calcite and the simultaneous reduction in portlandite content, consistent with the reaction between CO<sub>2</sub> and Ca(OH)<sub>2</sub>, as observed in earlier studies [40,41]. Based on the TGA results, the carbonation efficiency was estimated by comparing the experimentally measured CaCO<sub>3</sub> content with the theoretical value expected from complete carbonation of portlandite. In the reference mix (M1), the available 13.5 wt% of Ca(OH)2 would theoretically yield 18.3 wt% of CaCO3 upon full conversion. The measured CaCO<sub>3</sub> content in the carbonated mixes indicated efficiencies of approximately 66% for M2, 45% for M4 and M6, and only 16% for M8. These results confirm that carbonation was most effective in the simpler systems and progressively hindered by fiber-induced diffusion barriers and competing pozzolanic competition in multicomponent blends. Moreover, internal carbonation contributed to pH reduction, which is advantageous for mitigating fiber degradation, but it may affect hydration equilibrium and sulfate phase stability [31,42].

The variations in AFt and AFm contents reflect the sensitivity of sulfate-bearing phases to carbonation and pozzolanic reactions. The depletion of portlandite and pH reduction in the carbonated systems likely promoted the conversion of ettringite to monosulfate and amorphous alumina–silicate phases, consistent with the thermodynamic instability of AFt under lower Ca<sup>2+</sup> availability [43]. This partial transformation may have contributed to matrix densification through secondary gel formation, but also reduced the sulfate-buffering capacity, potentially influencing long-term stability and strength development [44,45].

This reaction serves as a secondary densification mechanism. It works synergistically with the primary reaction—the precipitation of calcite from portlandite carbonation—to refine the pore structure. The combined effect results in the observed microstructural densification and enhanced mechanical performance. Specifically, mix M2 achieved a compressive strength of 47.5 MPa, approximately 8% higher than the reference mix M1 (44 MPa), directly attributed to this dual-phase refinement. Thus, in this context, the AFt/AFm destabilization acts as an accelerated microstructural refinement process that ultimately enhances matrix compactness and compressive strength.

Calcined clay played a complementary role by contributing to long-term strength development and pore structure refinement via pozzolanic reactions. The increase in gel pore content and BET surface area, as observed especially in mixes without fibers (e.g., M5), aligns with prior studies emphasizing the role of metakaolin-rich clays in reducing permeability and enhancing C–A–S–H gel formation [32,46,47]. These findings also confirm that the combined use of calcined clay and carbonation can accelerate portlandite consumption, thereby modifying both chemical and physical aspects of the matrix [48,49].

The SEM micrographs (Figures 12 and 13) reveal pronounced degradation of wool fibers in M4 (CO<sub>2</sub> + wool), whereas fibers in M7 (calcined clay + wool) appear largely intact. Although both mortars exhibit similar bulk pH values at 28 days, the observed difference cannot be attributed to alkalinity alone. The internal carbonation applied in M4 likely created short-lived, CO<sub>2</sub> rich microenvironments during mixing and early hydration, resulting in localized acidification and keratin hydrolysis at the fiber surface [31,42,50]. This transient effect is not captured by the later pH measurement but could explain the severe deterioration visible in Figure 12. In addition, SEM-EDS and XRD analyses confirmed extensive CaCO<sub>3</sub> formation in carbonated mixes. The precipitation of sharp, plate-like calcite crystals at the fiber-matrix interface could mechanically damage the fibers or hinder stress transfer, contributing to the fragmented morphology [31]. The densified carbonated matrix in M4 may also have restricted the fibers and increased local shrinkage stresses, further promoting degradation [51,52]. Conversely, M7, without CO<sub>2</sub> addition, exhibited higher porosity and a more homogeneous C-A-S-H gel from calcined clay hydration, which likely provided a less aggressive and more compliant environment for the fibers [4,48]. Thus, the fiber integrity in M7 arises from the absence of early carbonation and the more compatible interfacial chemistry, despite having the same pH as M4.

In the most complex blend (i.e., M8), the combined use of dry ice, calcined clay, and wool fibers resulted in the lowest compressive strength and increased porosity, indicating chemical incompatibilities and structural disruption. The simultaneous action of carbonation and pozzolanic reactions led to almost complete depletion of portlandite ( $\approx$ 1.7 wt%), as confirmed by TGA, while the relatively low calcite content suggested restricted CO<sub>2</sub> transport through a heterogeneous pore network [53]. BET and MIP results also revealed increased total porosity and poor matrix densification, which corresponded with SEM observations of degraded fibers and voided interfaces [50,51]. Although the measured pH values remained within the typical alkaline range (12.0-12.5), the coexistence of carbonation and pozzolanic reactions likely generated local pH gradients and transient micro-environments detrimental to fiber stability [50,52]. The degradation observed under SEM was therefore not attributed to uniformly high alkalinity but to chemical heterogeneity and interfacial instability within the matrix, where the combined depletion of portlandite and altered ion concentrations may have accelerated the hydrolysis of wool keratin [52,53]. These coupled processes led to a discontinuous microstructure and pronounced strength loss, highlighting the antagonistic interactions among carbonation, pozzolanic reaction, and fiber inclusion. Similar mechanisms, pore blocking, limited CO<sub>2</sub> diffusion, and instability of hydration and carbonation products, have been reported in hybrid fiber-cement systems [54].

The correlations between portlandite content and pH (Figure 15) highlight the importance of alkalinity control in designing multicomponent mortars. The slight pH decreases from M1 to M8 (12.5–12.0) falls within instrumental uncertainty, yet it indicates a general trend of reduced alkalinity associated with concurrent carbonation and pozzolanic reactions. As reported in previous studies [55], minor variations in pH measurements may arise from specimen preparation and testing conditions. While moderate pH reduction may improve fiber durability, excessive portlandite depletion can hinder hydration or ettringite formation [46]. Moreover, the inverse correlation between BET surface area and compressive strength suggests that excessive porosity, caused by fiber addition or incomplete matrix densification, can offset the benefits of these chemical modifications [51].

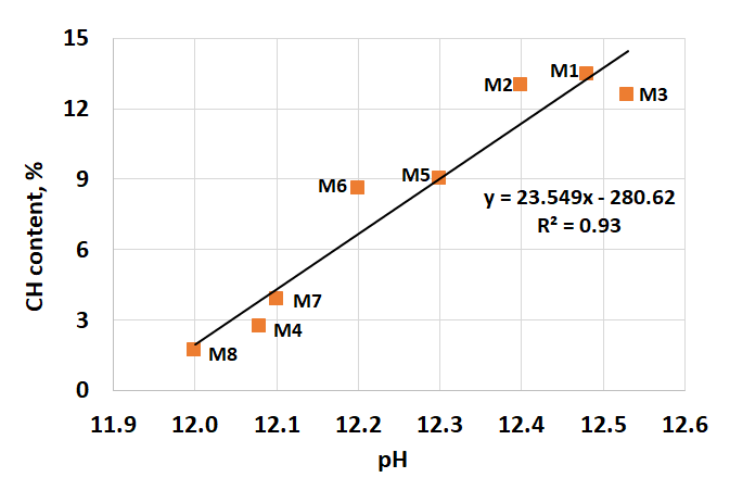


**Figure 15.** The relationship between portlandite content and pH value in the mortars investigated in this project.

Overall, this study confirms the feasibility of combining internal carbonation and pozzolanic additives to produce low-carbon cementitious systems, while also underscoring the need to address compatibility challenges with natural fibers. A trade-off exists between improved sustainability and mechanical performance, which must be managed through targeted mix design and material selection.

# 6. Conclusions

This study explored the structural behavior and microstructural development of cement mortars modified with dry ice, calcined clay, and sheep wool fibers, aiming to enhance sustainability without compromising performance. The following conclusions highlight all the findings relevant to structural engineering applications:

- Internal carbonation via dry ice increased compressive strength by approximately 8% compared to the reference mix and contributed to pore structure refinement, confirming its viability for developing low-carbon cementitious systems.
- Calcined clay, used as a 15–30% cement replacement, enhanced durability by stabilizing hydration products and refining the pore network, leading to a ~12% reduction in total pore volume and a higher gel-pore fraction (<10 nm).</li>
- Sheep wool fibers improved flexural toughness and post-cracking performance by more than 40%, validating their crack-bridging effect. However, SEM observations revealed degradation in high-pH or carbonated environments, which reduced longterm mechanical integrity. Additionally, fiber-induced porosity partially counteracted matrix densification.

 Microstructural analysis confirmed the complex interactions between carbonation, hydration, and fiber integrity, emphasizing the need to control chemical compatibility when designing multicomponent eco-mortars.

- To maximize strength and durability, fiber inclusion should be avoided when both dry
  ice and calcined clay are used, as their simultaneous application (M8) led to the lowest
  compressive strength (~30 MPa) and increased porosity.
- pH control and portlandite content were identified as key parameters influencing performance. While moderate pH reduction supports fiber stability, excessive portlandite depletion can hinder the formation of hydration products such as ettringite, whereas overly high alkalinity accelerates fiber degradation.
- The outcomes of this study indicate that internally carbonated and calcined clay-modified mortars have strong potential for real-world applications in prefabricated panels, eco-efficient repair mortars, and non-structural building components, where early strength development, durability, and reduced carbon footprint are critical. When combined with properly surface-treated natural fibers, such systems could contribute to the advancement of biogenic and circular construction materials, aligning with the goals of sustainable and low-emission building technologies.

Future research should focus on improving the alkaline resistance of natural fibers through surface modification techniques such as silane or epoxy coatings, plasma or alkali pre-treatments, and mineral-based coatings (e.g., silica or alumina layers), which have shown potential to enhance durability and interfacial adhesion in cementitious matrices. Further investigations should also explore alternative supplementary cementitious materials, life-cycle assessments of multicomponent eco-mortars, and full-scale applications, particularly in prefabricated façade elements and repair mortars, where carbon reduction and early strength are critical design priorities.

**Author Contributions:** Conceptualization, D.J.-N. and A.P.F.; Resources A.P.F.; Investigation, D.J.-N.; P.L.; A.B.; M.O. and A.P.F.; Formal analysis, D.J.-N.; D.A. and A.P.F.; Data curation, D.J.-N. and A.P.F.; Supervision, D.J.-N. and A.P.F.; Writing—original draft, D.J.-N. and A.P.F.; Writing—review and editing, D.J.-N.; P.L.; M.O.; A.B.; D.A. and A.P.F. All authors have read and agreed to the published version of the manuscript.

Funding: This research received no external funding.

Institutional Review Board Statement: Not applicable.

Informed Consent Statement: Not applicable.

Data Availability Statement: Data will be made available on request.

**Acknowledgments:** The authors would like to thank the Built laboratory of Buzzi cement company for providing the materials used in this research project.

Conflicts of Interest: The authors declare no conflicts of interest. The funders had no role in the design of the study; in the collection, analyses, or interpretation of data; in the writing of the manuscript; or in the decision to publish the results.

#### **Abbreviations**

The following abbreviations are used in this manuscript:

SCM Supplementary cementitious materials

 $\begin{array}{ll} f_t & Flexural \, strength \\ f_c & Compressive \, strength \\ A_F & Flexural \, toughness \\ C-S-H & Calcium \, silicate \, hydrate \end{array}$ 

C-A-S-H Calcium-alumino-silicate hydrate

LC<sup>3</sup> Limestone-calcined clay
C<sub>3</sub>A Tricalcium aluminate
C<sub>4</sub>AF Tetracalcium aluminoferrite

XRD X-ray Diffraction LOI Loss on ignition

SEM Scanning Electron Microscopy

AFt Ettringite
AFm Monosulfate

#### References

1. Andrew, R.M. Global CO<sub>2</sub> Emissions from Cement Production. Earth Syst. Sci. Data 2018, 10, 195–217. [CrossRef]

- 2. Zhang, D.; Ghouleh, Z.; Shao, Y. Review on Carbonation Curing of Cement-Based Materials. *J. CO*<sub>2</sub> *Util.* **2017**, 21, 119–131. [CrossRef]
- 3. Xuan, M.-Y.; Lee, S.; Hu, H.; Wang, X.-Y. Adding Dry Ice into Ultra-High-Performance Concrete to Enhance Engineering Performances and Lower CO<sub>2</sub> Emissions. *Constr. Build. Mater.* **2023**, 392, 131858. [CrossRef]
- 4. Jaskulski, R.; Jóźwiak-Niedźwiedzka, D.; Yakymechko, Y. Calcined Clay as Supplementary Cementitious Material. *Materials* **2020**, 13, 4734. [CrossRef] [PubMed]
- 5. Antoni, M.; Rossen, J.; Martirena, F.; Scrivener, K. Cement Substitution by a Combination of Metakaolin and Limestone. *Cem. Concr. Res.* **2012**, 42, 1579–1589. [CrossRef]
- 6. Cheah, C.B.; Liew, J.J.; Khaw, K.L.P.; bin Md Akil, H.; Alengaram, U.J. Calcined Clay as a Low-Carbon Cementitious Material: Comprehensive Review of Treatment Method, Properties, and Performance in Concrete. *Clean. Waste Syst.* **2025**, *11*, 100323. [CrossRef]
- 7. Bhagath Singh, G.V.P.; Scrivener, K.L. Investigation of Phase Formation, Microstructure and Mechanical Properties of LC3 Based Autoclaved Aerated Blocks. *Constr. Build. Mater.* **2022**, 344, 128198. [CrossRef]
- 8. Maia Pederneiras, C.; Veiga, R.; de Brito, J. Rendering Mortars Reinforced with Natural Sheep's Wool Fibers. *Materials* **2019**, 12, 3648. [CrossRef]
- 9. Fantilli, A.P.; Jóźwiak-Niedźwiedzka, D. Influence of Portland Cement Alkalinity on Wool Reinforced Mortar. *Proc. Inst. Civil. Eng.-Constr. Mater.* **2020**, 174, 172–181. [CrossRef]
- 10. Ardanuy, M.; Claramunt, J.; Toledo Filho, R.D. Cellulosic Fiber Reinforced Cement-Based Composites: A Review of Recent Research. *Constr. Build. Mater.* **2015**, *79*, 115–128. [CrossRef]
- 11. Wang, Y.-S.; Cho, H.-K.; Wang, X.-Y. Mixture Optimization of Sustainable Concrete with Silica Fume Considering CO<sub>2</sub> Emissions and Cost. *Buildings* **2022**, *12*, 1580. [CrossRef]
- 12. Tipu, R.K.; Rathi, P.; Pandya, K.S.; Panchal, V.R. Optimizing Sustainable Blended Concrete Mixes Using Deep Learning and Multi-Objective Optimization. *Sci. Rep.* **2025**, *15*, 16356. [CrossRef]
- 13. Marandi, N.; Shirzad, S. Sustainable Cement and Concrete Technologies: A Review of Materials and Processes for Carbon Reduction. *Innov. Infrastruct. Solut.* **2025**, *10*, 408. [CrossRef]
- 14. Wang, Y.; He, F.; Yang, L. Influence of Dry Ice on the Performance of Portland Cement and Its Mechanism. *Constr. Build. Mater.* **2018**, *188*, 898–904. [CrossRef]
- Yang, F.; Lai, C.; Liu, L.; Chen, Z.; Jia, H.; Zhu, J.; Jiang, Z.; Shi, C.; Liu, J. A New Method for Improving the Resistance of Cement-Based Materials to Carbonic Acid Water Corrosion: Carbonation Curing and Further Water Curing. Constr. Build. Mater. 2024, 422, 135733. [CrossRef]
- El-Hassan, H.; Shao, Y.; Ghouleh, Z. Reaction Products in Carbonation-Cured Lightweight Concrete. J. Mater. Civil Eng. 2013, 25, 799–809. [CrossRef]
- 17. Zhang, D.; Cai, X.; Shao, Y. Carbonation Curing of Precast Fly Ash Concrete. J. Mater. Civ. Eng. 2016, 28, 04016127. [CrossRef]
- 18. Fantilli, A.P.; Calvi, R.; Quieti, E.; Radavelli, P.L. Carbon Dioxide: A Raw Material for Cementitious Mortar. Mater. Proc. 2021, 5, 2.
- 19. Hu, C.; Shen, K.; Qin, Y.; Qian, X.; Wang, F. Sustainable MgO-Calcined Clay Cementitious Material: Reaction Mechanism, Strength Development and Performance Enhancement via Initial CO<sub>2</sub> Stirring. *Sustain. Mater. Technol.* **2024**, 40, e00911. [CrossRef]
- Mastali, M.; Abdollahnejad, Z.; Pacheco-Torgal, F. Carbon Dioxide Sequestration of Fly Ash Alkaline-Based Mortars Containing Recycled Aggregates and Reinforced by Hemp Fibres. Constr. Build. Mater. 2018, 160, 48–56. [CrossRef]
- 21. Ravikumar, D.; Zhang, D.; Keoleian, G.; Miller, S.; Sick, V.; Li, V. Carbon Dioxide Utilization in Concrete Curing or Mixing Might Not Produce a Net Climate Benefit. *Nat. Commun.* **2021**, *12*, 855. [CrossRef]
- 22. Barbhuiya, S.; Nepal, J.; Das, B.B. Properties, Compatibility, Environmental Benefits and Future Directions of Limestone Calcined Clay Cement (LC3) Concrete: A Review. *J. Build. Eng.* **2023**, *79*, 107794. [CrossRef]

23. Usanga, I.N.; Ikeagwuani, C.C.; Okafor, F.O.; Ambrose, E.E. Exploration of Calcined Clays and Nanoclays as a Potential Construction Material for Sustainable Development: A Comprehensive and State-of-the-Art Review. *Road Mater. Pavement Des.* **2024**, *26*, 887–920. [CrossRef]

- 24. Gartner, E.; Hirao, H. A Review of Alternative Approaches to the Reduction of CO<sub>2</sub> Emissions Associated with the Manufacture of the Binder Phase in Concrete. *Cem. Concr. Res.* **2015**, *78*, 126–142. [CrossRef]
- 25. Abbas, Y.M.; Khan, M.I.; Abellan-Garcia, J.; Castro-Cabeza, A. Synergizing Metakaolin and Waste-Glass for Sustainable and Functional UHPCC– a Central Composite Design and Ecological Footprint Assessment. J. Build. Eng. 2024, 95, 110249. [CrossRef]
- 26. Suescum-Morales, D.; Fernández, D.C.; Fernández, J.M.; Jiménez, J.R. The Combined Effect of CO<sub>2</sub> and Calcined Hydrotalcite on One-Coat Limestone Mortar Properties. *Constr. Build. Mater.* **2021**, 280, 122532. [CrossRef]
- 27. Alyousef, R.; Mohammadhosseini, H.; Ebid, A.A.K.; Alabduljabbar, H. An Integrated Approach to Using Sheep Wool as a Fibrous Material for Enhancing Strength and Transport Properties of Concrete Composites. *Materials* **2022**, *15*, 1638. [CrossRef]
- 28. Jóźwiak-Niedźwiedzka, D.; Fantilli, A.P. Wool-Reinforced Cement Based Composites. *Materials* **2020**, *13*, 3590. [CrossRef] [PubMed]
- 29. Fantilli, A.P.; Jóźwiak-Niedźwiedzka, D. The effect of hydraulic cements on the flexural behavior of wool reinforced mortars. *Acad. J. Civ. Eng.* **2019**, *37*, 287–292.
- 30. Tonoli, G.H.D.; Santos, S.F.; Joaquim, A.P.; Savastano, H. Effect of Accelerated Carbonation on Cementitious Roofing Tiles Reinforced with Lignocellulosic Fibre. *Constr. Build. Mater.* **2010**, 24, 193–201. [CrossRef]
- 31. Pizzol, V.D.; Mendes, L.M.; Frezzatti, L.; Savastano, H., Jr.; Tonoli, G.H.D. Effect of Accelerated Carbonation on the Microstructure and Physical Properties of Hybrid Fiber-Cement Composites. *Miner. Eng.* **2014**, *59*, 101–106. [CrossRef]
- 32. El-Hassan, H. Accelerated Carbonation Curing as a Means of Reducing Carbon Dioxide Emissions. In *Cement Industry—Optimization, Characterization and Sustainable Application*; IntechOpen: London, UK, 2021.
- 33. García, G.; Cabrera, R.; Rolón, J.; Pichardo, R.; Thomas, C. Natural Fibers as Reinforcement of Mortar and Concrete: A Systematic Review from Central and South American Regions. *J. Build. Eng.* **2024**, *98*, 111267. [CrossRef]
- 34. Ahmad, J.; Zhou, Z. Mechanical Properties of Natural as Well as Synthetic Fiber Reinforced Concrete: A Review. *Constr. Build. Mater.* **2022**, 333, 127353. [CrossRef]
- 35. Li, Y.; Han, D.; Wang, H.; Lyu, H.; Zou, D.; Liu, T. Carbonation Curing of Mortars Produced with Reactivated Cementitious Materials for CO<sub>2</sub> Sequestration. *J. Clean. Prod.* **2023**, *383*, 135501. [CrossRef]
- 36. Haq, I.U.; Bibi, T.; Nawaz, A.; Khalid, H.R.; Elahi, A. Calcined Clay–Substituted Sustainable Cement Binders: A Holistic Review. *Environ. Sci. Pollut. Res.* **2025**, 32, 11317–11349. [CrossRef] [PubMed]
- 37. *PN-EN 196-1*; Methods of Testing Cement—Determination of Strength. Polish Committee for Standardization: Warsaw, Poland, 2016; pp. 1–33.
- 38. Papadakis, V.G. Effect of Supplementary Cementing Materials on Concrete Resistance against Carbonation and Chloride Ingress. *Cem. Concr. Res.* **2000**, 30, 291–299. [CrossRef]
- 39. von Greve-Dierfeld, S.; Lothenbach, B.; Vollpracht, A.; Wu, B.; Huet, B.; Andrade, C.; Medina, C.; Thiel, C.; Gruyaert, E.; Vanoutrive, H.; et al. Understanding the Carbonation of Concrete with Supplementary Cementitious Materials: A Critical Review by RILEM TC 281-CCC. *Mater. Struct.* 2020, 53, 136. [CrossRef]
- 40. Saeki, N.; Kurihara, R.; Ohkubo, T.; Teramoto, A.; Suda, Y.; Kitagaki, R.; Maruyama, I. Semi-Dry Natural Carbonation at Different Relative Humidities: Degree of Carbonation and Reaction Kinetics of Calcium Hydrates in Cement Paste. *Cem. Concr. Res.* **2025**, 189, 107777. [CrossRef]
- 41. Galan, I.; Glasser, F.P.; Baza, D.; Andrade, C. Assessment of the Protective Effect of Carbonation on Portlandite Crystals. *Cem. Concr. Res.* **2015**, 74, 68–77. [CrossRef]
- 42. da Silva, P.M.; Mendes, J.P.; Coelho, L.C.C.; de Almeida, J.M.M.M. Real-Time Monitoring of Cement Paste Carbonation with In Situ Optical Fiber Sensors. *Chemosensors* **2023**, *11*, 449. [CrossRef]
- 43. Kuzielová, E.; Slaný, M.; Žemlička, M.; Másilko, J. Accelerated Carbonation of Oil-Well Cement Blended with Pozzolans and Latent Hydraulic Materials. *J. Therm. Anal. Calorim.* **2023**, *148*, 9963–9977. [CrossRef]
- 44. Missana, T.; Almendros-Ginestà, O.; Colmenero, F.; Fernández, A.M.; García-Gutiérrez, M. Investigation of the Surface Charge Behaviour of Ettringite: Influence of PH, Calcium, and Sulphate Ions. *Heliyon* **2024**, *10*, e36117. [CrossRef]
- 45. Zhang, Y.; Zhang, Q.; Chang, J.; Yang, H.; Ding, S.; Liu, X.; Wu, K.; Zhao, Q. Modeling and Experimental Validation of Carbonation Mechanism of Ye'elimite-Gypsum-Water System. *Mater. Struct.* **2025**, *58*, 146. [CrossRef]
- 46. Dousti, A.; Beyki, H.; Shekarchi, M. Strength and Durability Performance of Mortars Incorporating Calcined Clay as Pozzolan in Comparison with Silica Fume. *J. Civil. Eng. Mater. Appl.* **2022**, *6*, 159–174.
- 47. Nguyen, Q.D.; Afroz, S.; Castel, A. Influence of Calcined Clay Reactivity on the Mechanical Properties and Chloride Diffusion Resistance of Limestone Calcined Clay Cement (LC3) Concrete. *J. Mar. Sci. Eng.* **2020**, *8*, 301. [CrossRef]

48. Bernal, S.A.; Provis, J.L.; Brice, D.G.; Kilcullen, A.; Duxson, P.; van Deventer, J.S.J. Accelerated Carbonation Testing of Alkali-Activated Binders Significantly Underestimates Service Life: The Role of Pore Solution Chemistry. *Cem. Concr. Res.* **2012**, 42, 1317–1326. [CrossRef]

- 49. Balestra, C.E.T.; Savaris, G.; Nakano, A.Y.; Schneider, R. Carbonation of Concretes Containing LC<sup>3</sup> Cements with Different Supplementary Materials. *Semin. Ciênc. Exatas Tecnol.* **2022**, *43*, 161–170. [CrossRef]
- 50. Wei, J.; Meyer, C. Degradation Rate of Natural Fiber in Cement Composites Exposed to Various Accelerated Aging Environment Conditions. *Corros. Sci.* **2014**, *88*, 118–132. [CrossRef]
- 51. Lilargem Rocha, D.; Tambara Júnior, L.; Marvila, M.; Pereira, E.; Souza, D.; de Azevedo, A. A Review of the Use of Natural Fibers in Cement Composites: Concepts, Applications and Brazilian History. *Polymers* **2022**, *14*, 2043. [CrossRef]
- 52. Amsalu Fode, T.; Chande Jande, Y.A.; Kivevele, T.; Rahbar, N. A Review on Degradation Improvement of Sisal Fiber by Alkali and Pozzolana for Cement Composite Materials. *J. Nat. Fibers* **2024**, *21*, 2335327. [CrossRef]
- 53. Li, Y.; Miao, L.; Dong, Z.; Jin, Y.; Liu, W.; Gao, F.; Li, Y. Carbonation and Chloride Resistance Characteristics of Self-Developed Limestone Calcined Clay Cement (LC3) Derived from Excavated Spoil. *Materials* **2025**, *18*, 2546. [CrossRef] [PubMed]
- 54. Rakhsh Mahpour, A.; Ventura, H.; Ardanuy, M.; Rosell, J.R.; Claramunt, J. The Effect of Fibres and Carbonation Conditions on the Mechanical Properties and Microstructure of Lime/Flax Composites. *Cem. Concr. Compos.* **2023**, *138*, 104981. [CrossRef]
- 55. Manso, S.; Aguado, A. A Review of Sample Preparation and Its Influence on Ph Determination in Concrete Samples. *Mater. Constr.* **2017**, *67*, e108. [CrossRef]

Disclaimer/Publisher's Note: The statements, opinions and data contained in all publications are solely those of the individual author(s) and contributor(s) and not of MDPI and/or the editor(s). MDPI and/or the editor(s) disclaim responsibility for any injury to people or property resulting from any ideas, methods, instructions or products referred to in the content.